DE83008430

DESIGN AND MODELING OF LOW-PRESSURE-DROP METHANATION REACTORS

DEPARTMENT OF ENERGY, PITTSBURGH, PA.
PITTSBURGH ENERGY TECHNOLOGY CENTER

1978

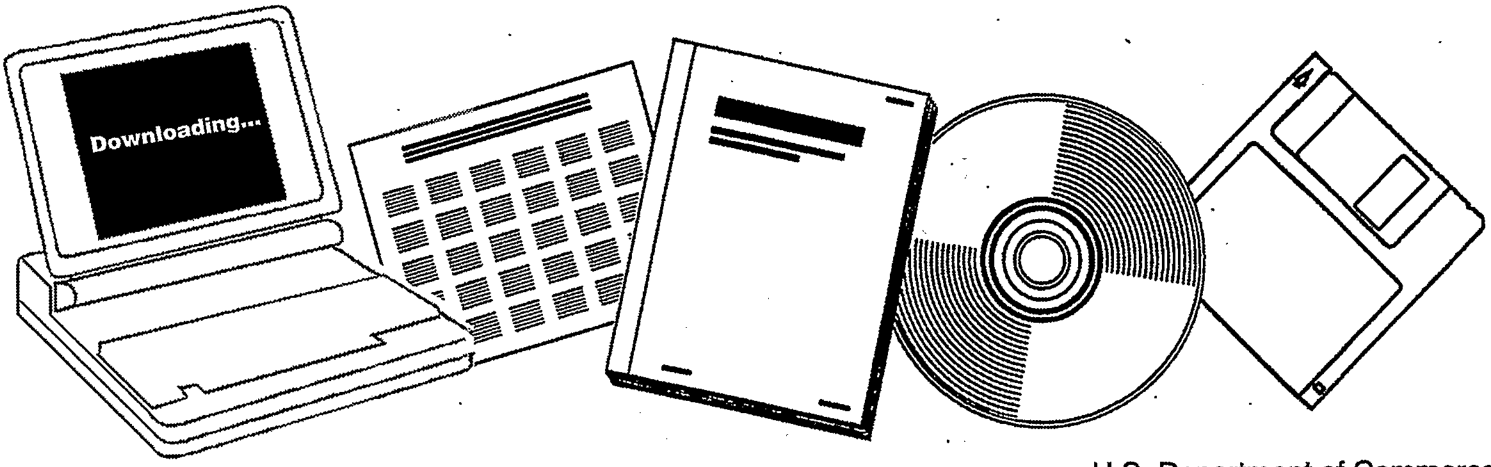

DE83008430

CONF-781110--18

DE83 008430

Design and Modeling of Low-Pressure-Drop Methanation Reactors

By

R. R. Schehl, (Speaker) and W. P. Haynes

Pittsburgh Energy Technology Center
U. S. Department of Energy
4800 Forbes Avenue
Pittsburgh, PA 15213

To be presented at the 71st Annual AIChE Meeting
Miami, Florida
November 1978

Design and Modeling of Low-Pressure-Drop Methanation Reactors

By

R. R. Schehl (Speaker) and W. P. Haynes

Pittsburgh Energy Technology Center
Department of Energy
Pittsburgh, PA 15213

This paper discusses the design and operation of low-pressure-drop methanation systems under development at the Pittsburgh Energy Technology Center. Mathematical models, supported by bench-scale studies, are outlined and their applicability to large-scale systems is tested with operating data from Process Development Units.

Introduction

At the Pittsburgh Energy Technology Center (PETC), emphasis has been placed on the development of a methanation system which has low-pressure-drop characteristics in order to minimize recycle compression costs and a design which maximizes recovery of the heat of reaction by generating high pressure steam. Three systems under investigation at PETC, the Hot Gas Recycle, Tube Wall and Hybrid methanation systems, have these qualifications. The Hot Gas Recycle process utilizes a parallel plate adiabatic reactor with the heat of reaction removed by partially cooling the hot product recycle. The heat of reaction is directly removed from the Tube Wall reactor by vaporizing Dowtherm at 375° C. The Hybrid system employs both methods of heat removal; the majority of the heat of reaction is removed from the reactor by generating 1200 psi steam while the remainder is carried away as sensible heat of the process gas.

Raney nickel catalyst, either flame-sprayed onto stainless steel substrates or cast into finned inserts, is used in these reactor systems. Other types of catalyst are being tested, but to date none has exhibited activity and life comparable to Raney nickel for our particular application. One year of operation has been demonstrated in a Process Development Unit with a Raney nickel catalyst.

Process Description

A simplified schematic flowsheet of the Hot Gas Recycle system is illustrated in Figure 1. Fresh feed gas is mixed with partially cooled, recycled product gas before entering the reactor at a temperature of 300° C. Temperature rise through the catalyst bed is limited to 100° C by controlling the recycle-to-feed-gas ratio. The major portion of reactor effluent is sent to a compressor and returned to the reactor inlet with the remainder going to a trim methanator. The hot recycle gas must be partially cooled by generating high pressure steam in order to provide the mixed feed gas temperature of 300° C at the reactor inlet. The catalyst bed consists of stainless steel, parallel plate grid assemblies. Raney nickel catalyst is flame-sprayed onto the plates before they are bolted together. Compressor costs are low in this system as a result of the catalyst bed design. Pressure drop across a bed of parallel plates is on the order of 1/15 that across a bed of pelleted catalyst at comparable space velocities. This permits the use of a single-stage, centrifugal hot gas recycle compressor. Other features of this system are the simplicity of design and operation and the recovery of the heat of reaction as high pressure steam.

The Tube Wall methanation concept takes advantage of the high heat transfer rates available by placing a thin coating of methanation catalyst in intimate contact with the surface of heat exchanger tubes. Figure 2 is a schematic flowsheet of the Tube Wall methanation process. Feed gas to the system is preheated to 300° C by heat exchange against the methanation reactor effluent. The methanation reaction is catalyzed on the inside tube surface of the shell and tube heat exchanger-reactor. The heat of reaction is removed by vaporizing Dowtherm on the shell side of the reactor 375° C. The Dowtherm vapor is condensed by generating high pressure steam and then returned to the reactor. The cooled product gas is sent to a trim methanator. The catalytic tube surface is prepared by flame spraying Raney nickel alloy directly onto the inside surface of the 2" diameter tubes to a thickness of .025". Activation of the catalyst is performed in situ by leaching the aluminum from the alloy with a caustic solution. The tube wall methanation concept has the advantages of requiring no product recycle and the recovery of the heat of reaction as high pressure steam.

The third type of methanation scheme developed by the Pittsburgh Energy Technology Center is a compromise between the Hot Gas Recycle and Tube Wall concepts. The reactor is similar in design to that used in the Tube Wall system; however, the catalyst is in the form of multi-finned inserts rather than coated onto the tube surface. The Hybrid concept is illustrated in Figure 3. As in the case of the Hot Gas Recycle system, the feed gas is mixed with partially cooled, recycled product gas and enters the reactor at 300° C. In the reactor, 70 to 80% of the heat of reaction is removed by generating 1200 psi steam on the shell side of the heat exchanger-reactor. The maximum catalyst temperature is limited to 400° C by controlling the amount of recycled hot product gas. Heat is removed from the catalyst via the process gas stream by convective heat transfer to the cooler tube wall. A portion of the reactor product is split off and sent to a trim methanator while the required amount of recycle is compressed hot before mixing with the feed gas. Once again, pressure drop across the reactor is negligible and a single-stage, centrifugal recycle compressor may be utilized. The Hybrid system requires only about half the amount of product recycle as the Hot Gas Recycle system and high pressure steam is generated directly in the reactor. Catalyst replacement would be much easier in the case of the Hybrid reactor than for the Tube Wall methanator.

Model Description

All of the systems described above have the common property that the methanation reaction is wall catalyzed, with the catalyst present in relatively thin layers and occupying a small fraction of the total reactor volume. Due to this commonality, the chemical and physical processes involved can be described pictorially in Figure 4. The stainless steel substrate is first grit-blasted to provide keyways which improve bonding of the catalyst alloy to the substrate. A thin coat (.004-.007 inches) of bonding material consisting of 95% Ni and 5% Al is first thermally sprayed onto the substrate. Subsequent to the bond coat, Raney nickel alloy powder (42 wt. % Ni and 58 wt. % Al, 80-200 mesh) is thermally deposited onto the surface until the desired thickness of about .023 inches is achieved. The alloy powder has been applied with both an oxy-hydrogen flame-spray torch and a plasma arc gun. The catalyst is activated by passing a 2 wt. percent aqueous solution of NaOH over the coating until approximately 70% of the aluminum in the Raney alloy is reacted. The extent of activation is determined by measuring the quantity of hydrogen which evolves according to 3 moles of H_2 for every 2 moles of Al reacted. After activation, the catalyst is rinsed with demineralized water to remove residual caustic and then maintained under hydrogen until being brought into service.

The reacting gas, flowing through the conduit in turbulent flow, is considered to be thoroughly mixed in the radial direction, i.e., there are no thermal or concentration gradients across the turbulent core. The reactants, CO and H_2, are transported across the laminar sublayer and are converted within the catalyst layer to methane and water.

$$CO + 3H_2 \rightarrow CH_4 + H_2O \qquad (1)$$

The rate of reaction will be uniform throughout the activated layer (thickness δ) provided there are no pore diffusion limitations. The exothermic heat of reaction, Q, liberated within the active catalyst layer is removed by either a q_1 or q_2 mechanism, depending upon the particular methanation system. The heat is removed via q_2 in the Tube Wall methanator, since, in this case, the substrate is a heat exchanger tube with coolant opposite the catalyst coating. In the Hot Gas Recycle and Hybrid system the heat is removed by convective heat transfer to the turbulent gas which is at a lower temperature than the catalyst.

Neglecting for the moment heat transfer effects, the global reaction rate at any position along the length of the reactor is specified by the catalyst temperature, T_c, bulk stream reactant concentrations, $\{C_i\}$, the thickness of the activated catalyst layer, δ, and mass transfer coefficients, $\{k_{c_i}\}$. These variables are coupled through the intrinsic rate expression and the mass transfer equations. For example, for carbon monoxide consumption, the set of equations would become:

$$r_{co} = f(\{\tilde{C}_i\}, T_c, \delta) \qquad (2)$$

$$j_{co} = k_{c_{co}} (C_{co} - \tilde{C}_{co}) \qquad (3)$$

$$j_{H_2} = k_{c_{H_2}} (C_{H_2} - \tilde{C}_{H_2}) \qquad (4)$$

The molar fluxes of CH_4 and H_2O are not required to be specified, since, as will be shown below, r_i is not a function of CH_4 and H_2O concentration. If there is external mass transfer control $\{\tilde{C}_i\}$ will, of course, be less than $\{C_i\}$. In order to develop an empirical intrinsic rate correlation, external transport effects must be eliminated since $\{\tilde{C}_i\}$ are not directly measurable. This can most conveniently be achieved through the use of a Berty reactor, due to the high internal recycle rates. The Berty reactor used to obtain kinetic data for a rate correlation is shown in Figure 5. The reactor was modified so that a 1/8" thermocouple well could be positioned along the axis of the draft tube. A coupon (1/2" x 1-3/4" x 1/8") was welded onto the end of the thermocouple well and coated with flame-sprayed Raney nickel alloy. This configuration permits rates to be measured with catalyst in the same physical state as is used in Process Development Units and, at the same time, allows for direct measurement of the catalyst temperature.

Figure 6 is an Arrhenius diagram of rate data obtained in the temperature range 240° C - 400° C at 20° C intervals. Data from two consecutive tests with different catalyst coupons are shown to indicate reproducibility. Flows were controlled to yield the same reactant concentrations (1% CO, 4-5% H_2) within the reactor for each data point. The straight line fit of the data below 330° C indicates that the rate is reaction controlled in this range. Above 330° C, the data indicate a transition to external diffusion control. The activation energy for the methanation reaction in the reaction controlled range was calculated to be 20 Kcal/gm-mole. In order to avoid heat and mass transfer effects, data for the kinetic correlations were obtained at 300° C. Carbon monoxide partial pressure was varied from .5 to 25 psi while hydrogen ranged from 5 to 85 psi. The remainder of the gas was methane and a small amount of water (10-30 psi). Methane was used as a diluent to the feed gas; however, water was present only as a result of product of reaction. A parity plot of the experimentally measured rate against the rate calculated from the multiple regression equation is shown in Figure 7. The multiple correlation coefficient for the fit was 0.986. By varying the amount of methane diluent in the feed gas, methane concentrations were varied from 5 to 95% with no effect on the reaction rate. It was assumed, therefore, that the intrinsic reaction rate was dependent only upon the CO and H_2 concentrations. The data shown in Figure 7 was obtained with an activated catalyst thickness of 0.0192 inches. Different activation depths were investigated, and, as expected, in the reaction controlled range the rate was linearly dependent on the thickness of the activated layer. Piecing this information together, Equation 2 then becomes:

$$-r_{co} = 0.22 \times 10^{9}\ \delta\ e^{-20,000/RT_c^a}\ \tilde{C}_{CO}^{.26}\ \tilde{C}_{H_2}^{.46} \qquad (5)$$

Hot Gas Recycle System

The Hot Gas Recycle Process Development Unit has been previously described (1) and the details will not be reiterated. The heat of reaction is removed from the catalyst-coated plates by convective heat transfer to the bulk gas stream in this system and is carried away as sensible heat to the recycled product gas. At steady state conditions there is no net change in reactant concentrations at the catalyst surface; thus, the rate of reaction must equal the rate at which CO and H_2 are transported to the surface. Hence:

$$-r_{co} = 0.22 \times 10^{9}\ \delta\ e^{-20,000/RT_c^a}\ \tilde{C}_{CO}^{.26}\ \tilde{C}_{H_2}^{.46} \qquad (6)$$

$$j_{co} = -r_{co} = k_{c_{co}}\ (C_{co} - \tilde{C}_{co}) \qquad (7)$$

$$j_{H_2} = -3r_{co} = k_{c_{H_2}}\ (C_{H_2} - \tilde{C}_{H_2}) \qquad (8)$$

$$-r_{co}H = C_pM\ \frac{dT_G}{da} \qquad (9)$$

$$-r_{co}H = h\ (T_c - T_G). \qquad (10)$$

A compartments, or tanks-in-series, model is used to calculate concentration and temperature profiles as a function of distance through the reactor. Equations (6), (7), and (8) are solved simultaneously within each backmixed compartment using the catalyst temperature calculated in the previous compartment. Equation (9) is used to obtain the temperature of the gas in the subsequent compartment and equation (10) yields the catalyst temperature in the next compartment. The water-gas shift reaction:

$$CO + H_2O \rightleftarrows CO_2 + H_2 \qquad (11)$$

is neglected since little CO_2 is observed under our operating conditions and rates of formation of H_2, CH_4 and H_2O may be calculated from the stoichiometry of Equation(1). Results of the application of this model to a test in the Process Development Unit are shown in Figure 8. The solid circles in Figure 8 indicate experimentally measured gas temperatures, the solid line is the calculated gas temperature profile, and the dashed line is the calculated catalyst temperature profile. Good agreement is observed between calculated and observed gas temperatures; however, since catalyst temperatures could not be measured in this reactor, the predicted catalyst temperature is not confirmed.

Tube Wall System

The design and operation of the Tube Wall Process Development Unit has been discussed elsewhere (2). The heat of reaction is removed from the catalyst principally by conduction through the heat exchanger tube and then by nucleate boiling of Dowtherm on the shell side of the vessel. As will be seen below, a small portion of the heat leaves as sensible heat to the process gas. Equations (6), (7) and (8) remain the same for the Tube Wall reactor with, of course, the appropriate mass transfer coefficients. The equations describing heat transfer are as follows.

$$q_1 = h(T_c - T_G) = C_P M \frac{dT_G}{da} \qquad (12)$$

$$q_2 = \frac{k}{t}(T_c - T_W) = h_D(T_W - T_D) \qquad (13)$$

$$-r_{co}H = q_1 + q_2 \qquad (14)$$

A compartments model is again used to predict concentrations and temperature profiles through the reactor. Equations (6), (7) and (8) yield the rate of CO consumption within a given compartment while equation (12) relates the rate change in the sensible heat of the process gas to the convective heat transfer rate from the catalyst surface. Equation (13) is the rate of heat transfer to the Dowtherm coolant and equation (14) is just an energy balance.

Figure 9 illustrates the calculated temperature profiles for the Tube Wall reactor. The process gas enters the reactor at 350° C, heats rapidly to 380° C, and then drops off to about 375° C at the exit. The calculated catalyst temperature is 405° C at the inlet and then decreases monotonically through the reactor. Poor agreement of the observed temperature, indicated by solid circles, with either catalyst or gas temperature is observed. This is not unexpected since, although the thermocouple wells were positioned so that they were against the catalyst surface, the observed temperature is very likely some average of the actual catalyst and bulk gas temperatures. Figure 10 shows a comparison of predicted CO concentration profiles with experimentally measured values.

Hybrid System

A test, one year in duration, of the Hybrid system was discussed at the 84th AIChE Meeting in Atlanta (3). The catalyst inserts used in this test consisted of solid castings of Raney nickel alloy instead of flame-sprayed alloy coatings. Since only a thin layer of the outside portion of the castings was activated, however, the same kinetic model that was used for the Hot Gas Recycle and Tube Wall systems may be applied here. The heat generated on the catalyst surface goes to the turbulent gas core by convective heat transfer. Within each compartment, a portion of the heat leaves as sensible heat of the process gas and a portion by convective heat transfer to the wall of the heat exchanger tube. Radiation heat transfer is neglected due to the relatively low temperatures. Hence, in addition to Equations (6), (7), and (8), the following heat transfer and energy balance equations are written.

$$-r_{co} H = h(T_c - T_G) \qquad (15)$$

$$h(T_G - T_W') = \frac{k}{t} (T_W' - T_W) = h_D(T_W - T_D) \qquad (16)$$

$$C_P M \frac{dT_G}{da} da = -r_{co} H \, da - h \, (T_G - T_W')da' \qquad (17)$$

Equation (15) equates the rate of heat transfer from the catalyst surface to the rate of heat generation. The rate that heat is transferred from the turbulent gas core to the Dowtherm coolant is described by Equation (16) while Equation (17) is an energy balance equation yielding the rate increase of the sensible heat of the gas. Dowtherm vaporization rather than steam generation was used in the Process Development Unit.

Figure 11 shows a comparison of calculated and measured gas and catalyst temperature profiles for three different exposure velocities. Exposure velocity is the ratio of scfh of H_2 + CO feed to the superficial surface area of catalyst measured in ft^2. Model agreement at the 10 scfh/ft^2 exposure velocity is rather poor. This is very likely due to the fact that the Reynold's number at this flow was only 1900 and under laminar flow conditions would be out of range of the model. Figure 12 is a plot of CO mole fraction as a function of distance through the reactor. Gas stream compositions were measured at 21 inch intervals through the reactor. These data also represent operation at exposure velocities 10, 20 and 40 scfh/ft^2 of catalyst and were taken early in the run before any deactivation of the catalyst was evident. The points indicate experimentally measured values whereas the solid lines represent the profiles calculated from the model.

Deactivation

There are numerous possible mechanisms for the deactivation of Raney nickel when used as a methanation catalyst (4). The poisoning mechanism assumed here is that of the irreversible adsorption of compounds other than the principal reactants and products on the catalytically active sites. This is commonly referred to as type I, or independent poisoning. Following the work of Haynes (5), an irreversible Langmuir-Hinshelwood type of expression is assumed for the rate of formation of adsorbed poison:

$$r_P = k_P \, c_P \, (1 - W/W_s). \qquad (18)$$

In terms of the dimensionless groupings:

$$\psi = W/W_s$$

$$\phi = c_p/c_p^\circ \qquad (19)$$

$$\theta = k_p\ c_p^\circ \tau/W_s\ ,$$

The equation for the poisoning rate may be expressed as:

$$\frac{\partial\psi}{\partial\theta} = \phi\ (1-\psi). \qquad (20)$$

Equation (20) can be solved simultaneously with a differential mass balance of the poison species across an element of catalyst surface,

$$\frac{\partial c_p}{\partial a} + \frac{1}{V}\, r_p = 0, \qquad (21)$$

where V is the volumetric flow rate at operating temperature and pressure.

The following assumptions must be made if Equations (20) and (21) are to describe the temporal and spatial dependence of C_p in the reactor: (1) External mass transfer resistance is neglected. In other words, the poisoning is reaction controlled with the reaction rate given by Equation (20); (2) The catalyst is considered to be only an active superficial surface; (3) Volumetric contraction of the gas due to the methanation reaction is neglected. The spatial coordinate is taken to be the superficial catalyst surface area measured from the reactor inlet.

With the definitions $\lambda = a/a_o$ and $N_p = a_o K_p/V$, where a_o is the total superficial catalyst area, Equation (21) becomes:

$$\frac{\partial\phi}{\partial\lambda} + N_p\ \phi\ (1 - \psi) = 0. \qquad (22)$$

Equations (20) and (22) must be solved simultaneously for λ and θ. If the catalyst bed is initially free of adsorbed poison and the concentration of poison precursor in the feed remains constant with time, then the following boundary conditions are applicable:

$$\psi\ (0,\ \lambda) = 0 \qquad (23)$$

$$\phi\ (\theta,\ 0) = 1$$

The analytical solution of this system is rather tedious. It has, however, been solved in closed form by Bohart and Adams (6) and in more general terms by Amundson (7). The solution is:

$$\psi\ (\theta,\lambda) = (1-e^{-\theta})/[\ 1 + e^{-\theta}\ (e^{N_p\lambda} - 1)]. \qquad (24)$$

The function $\psi(\theta, \lambda)$ may be directly related to the catalyst activity at any point (τ, a) as follows:

$$A = A_{\text{initial}} (1-\psi) \qquad (25)$$

provided that the initial catalyst activity is uniform over the entire catalyst bed. Hence Equation 6 becomes:

$$-r_{CO} = 0.22 \times 10^9\ \delta\ e^{-20,000/RT_c^a}\ \tilde{C}_{CO}^{.26}\ \tilde{C}_{H_2}^{.46}\ (1-\psi). \qquad (26)$$

The deactivation factor $(1-\psi)$ has essentially two parameters which must be determined from experiment, as there are insufficient independent data to predict them a priori. Let these parameters be called p_1 and p_2, and be defined by:

$$p_1 = \theta/\tau = k_p\ \overset{\circ}{c}_p/W_s$$

$$p_2 = N_p\lambda/a = k_p/V.$$

These parameters have been evaluated by fitting the model to experimental gas stream temperature profiles measured at five different times during run HGR-15. The average values of the parameters determined by this procedure were then used to predict reactor performance throughout the entire test. Figure 13 illustrates the comparison of calculated gas temperature profiles with experimentally measured temperatures for several different times on stream.

Figure 14 shows a comparison of the calculated relative deactivation profile with measured carbon and sulfur concentrations on the catalyst for run HGR-15. The relative deactivation, $\psi(\tau,a)$, was calculated for the total time of operation, 1300 hours. Experimentally measured carbon and sulfur concentrations are normalized to unity at the reactor inlet. In effect, by thus normalizing, one is assuming that this is the amount of contaminant just sufficient to completely deactivate the catalyst. Figure 14 indicates reasonably good agreement between measured carbon concentrations and the curve predicted by the deactivation model.

Although the mathematical formalism for this deactivation model is derived from a type I mechanism, Figure 14 indicates that the possibility of some other mode of deactivation being chiefly responsible for the degradation of flame-sprayed Raney nickel should not be ruled out. For instance the type II parallel fouling mechanisms

$$2CO \rightarrow C + CO_2$$

$$XNi + 2CO \rightarrow Ni_xC + CO_2$$

which involve carbon monoxide as reactant might be expected to develop a deactivation profile similar to that predicted by Equation (24). The concentration of carbon monoxide is higher at the inlet portion of the bed, of course, and it is in this region that the catalyst is preferentially deactivated.

Nomenclature

a = catalyst surface area (ft^2)
a' = tube wall surface area (ft^2)
C = reactant concentration in bulk gas (lb mole/ft^3)
$\tilde{C}$ = reactant concentration at catalyst surface (lb mole/ft^3)
C_p = specific heat of gas (Btu/lb mole - °F)
c_p = poison concentration (lb mole/ft^3)
c_p° = poison concentration in feed (lb mole/ft^3)
E = activation energy (K cal/gm-mole)
h = heat transfer coefficient (Btu/hr-ft^2 - °F)
H = heat of reaction (Btu/lb mole)
j = molar flux (lb mole/hr-ft^2)
k = thermal conductivity of tube wall (Btu-ft/hr-ft^2-°F)
k_c = mass transfer coefficient (lb mole/hr-ft^2-concentration difference)
k_p = poisoning rate constant (ft/hr)
M = gas molar flowrate (lb mole/hr)
N_p = dimensionless constant
q = heat flux (Btu/hr-ft^2)
r = rate of conversion (lb mole/hr-ft^2 catalyst)
R = gas constant (cal/°K-gm mole)
t = tube wall thickness (ft)
T_c = catalyst temperature (°C)
T_c^a = absolute catalyst temperature (°K)
T_D = Dowtherm temperature (°C)
T_G = gas temperature (°C)
T_W = wall coolant side temperature (°C)
T_W' = wall gas side temperature (°C)
V = volumetric gas flow rate (ft^3/hr)
W = poison concentration on catalyst surface (lb mole/ft^2)
W_s = value of W corresponding to complete deactivation (lb mole/ft^2)

Nomenclature (cont)

δ = thickness of activated catalyst layer (ft)

θ = dimensionless time

λ = dimensionless surface area

τ = real time (hr)

ϕ = dimensionless concentration

ψ = dimensionless concentration

References

1. Haynes, W. P., R. R. Schehl, J. K. Weber, A. J. Forney, The Study of an Adiabatic Parallel Plate Methanation Reactor, I & EC Process Design and Development, 16, 113, 1977.

2. Pennline, H. W., R. R. Schehl, W. P. Haynes, Operation of a Tube Wall Methanation Reactor, Presented at Joint American Chemical Society - Chemical Institute of Canada Meeting, Symposium on Catalysis of Coal Conversion Processes, Montreal, Canada, May 29, 1977.

3. Pennline, H. W., R. R. Schehl, W. P. Haynes, Extended Operation of a PDU Methanation Reactor, Presented at the 84th AIChE National Meeting, Atlanta, GA, March 1, 1978.

4. Schehl, R. R., H. W. Pennline, A. J. Youngblood, M. J. Baird, J. P. Strakey, W. P. Haynes, Deactivation of Raney Nickel Methanation Catalyst, PERC/RI-77/10.

5. Haynes, H. W. Poisoning in Fixed Bed Reactors, Chem. Eng. Sci., 25, 1615, 1970.

6. Bohart, G. S., and E. Q. Adams, Some Aspects of the Behavior of Charcoal with Respect to Chlorine, J. Am. Chem. Soc., 42 523, 1920.

7. Amundson, N. R., A Note on the Mathematics of Adsorption in Beds, J. Phys. (Colloidal) Chem., 53, 1153, 1948.

Figure 1. Hot Gas Recycle Process

Figure 2. Tube Wall Process

Figure 3. Hybrid Process

Figure 4. View of catalyst gas interface

Figure 5. Berty reactor used for methanation kinetic studies

Figure 6. Arrhenius diagram for flame-sprayed Raney nickel

Figure 7. Parity plot illustrating the fit of experimental data to the kinetic regression equation.

Figure 8. Temperature profiles for a Hot Gas Recycle Process Development Unit.

Figure 9. Temperature profiles for a Tube Wall Process Development Unit.

Figure 10. Concentration profile for a Tube Wall Process Development Unit.

Figure 11. Temperature profiles for a Hybrid Process Development Unit for three different exposure velocities.

Figure 12. Concentration profiles for a Hybrid Process Development Unit for three different exposure velocities.

Figure 13. Gas temperature profiles of a Hot Gas Recycle Process Development Unit for different times on stream.

Figure 14. Poison profiles from Run HGR-15.

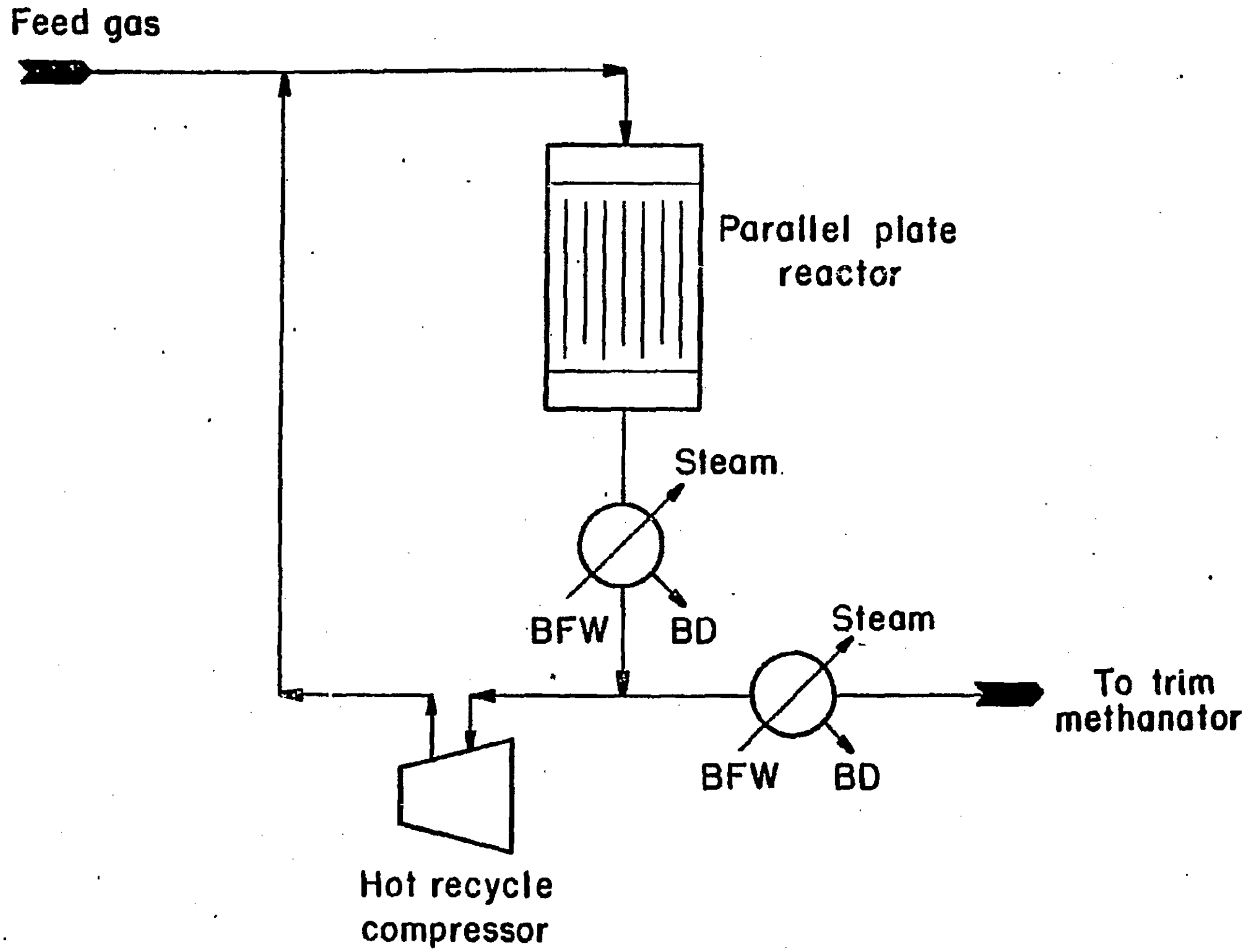

Figure 1. Hot Gas Recycle Process

5-31-78 L-16068

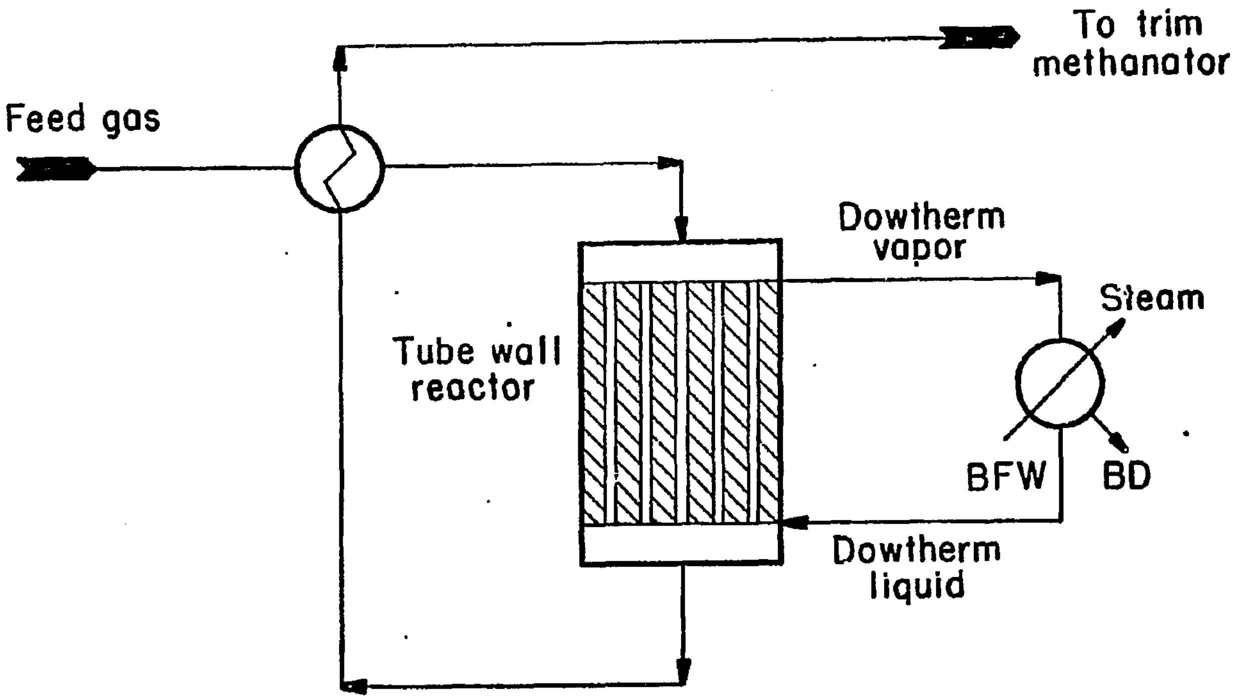

Figure 2. Tube Wall Process

9-30-77 L-15640

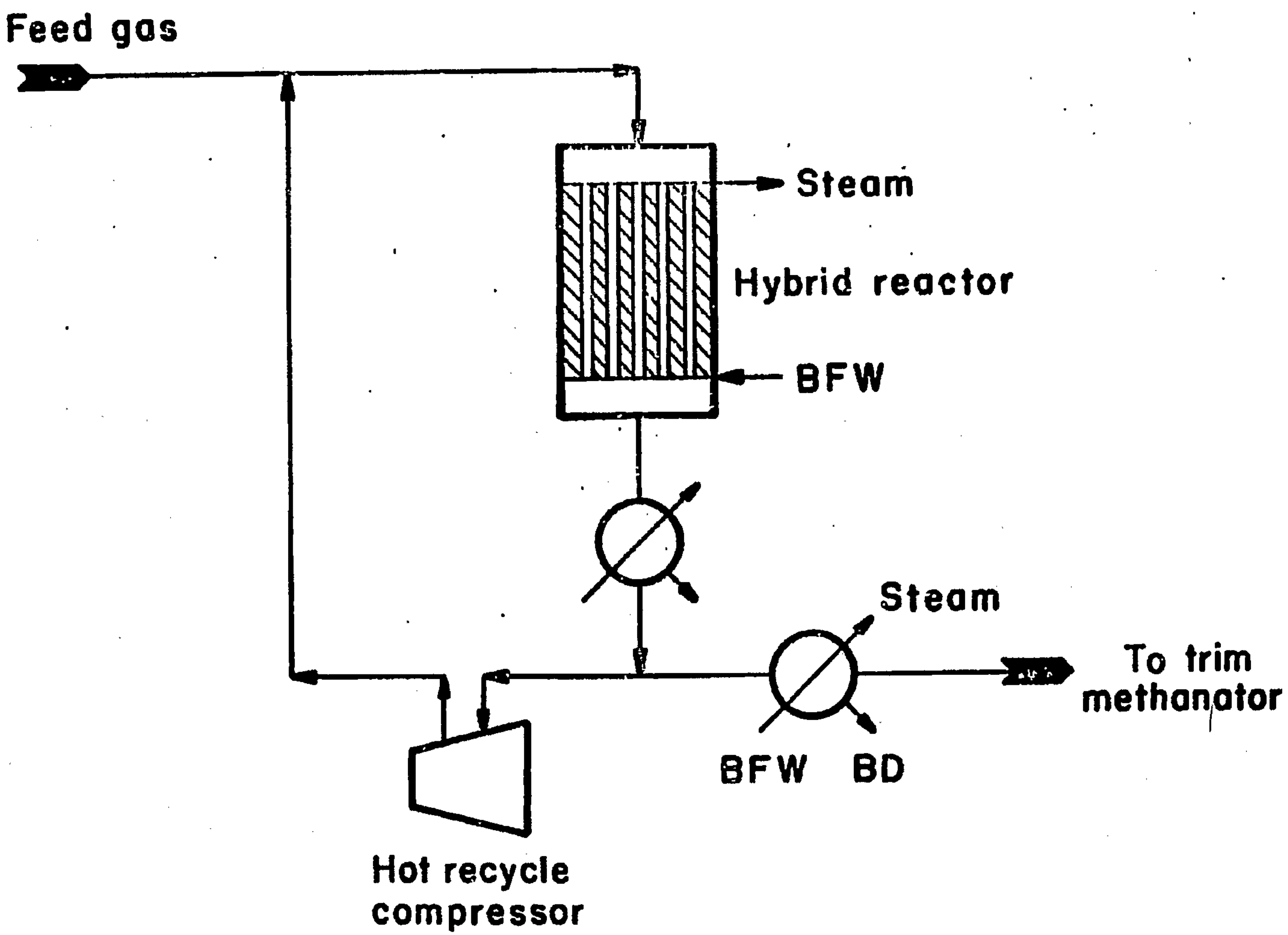

Figure 3. Hybrid Process

1-16-78 L-15803

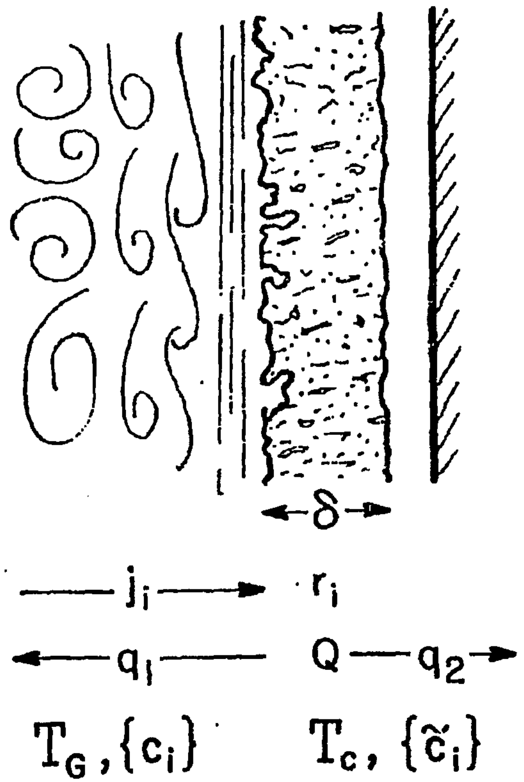

$$r_i = f(\{\tilde{c}_i\}, T_c, \delta)$$

$$j_i = k_{c_i}(c_i - \tilde{c}_i)$$

Figure 4. View of catalyst gas interface

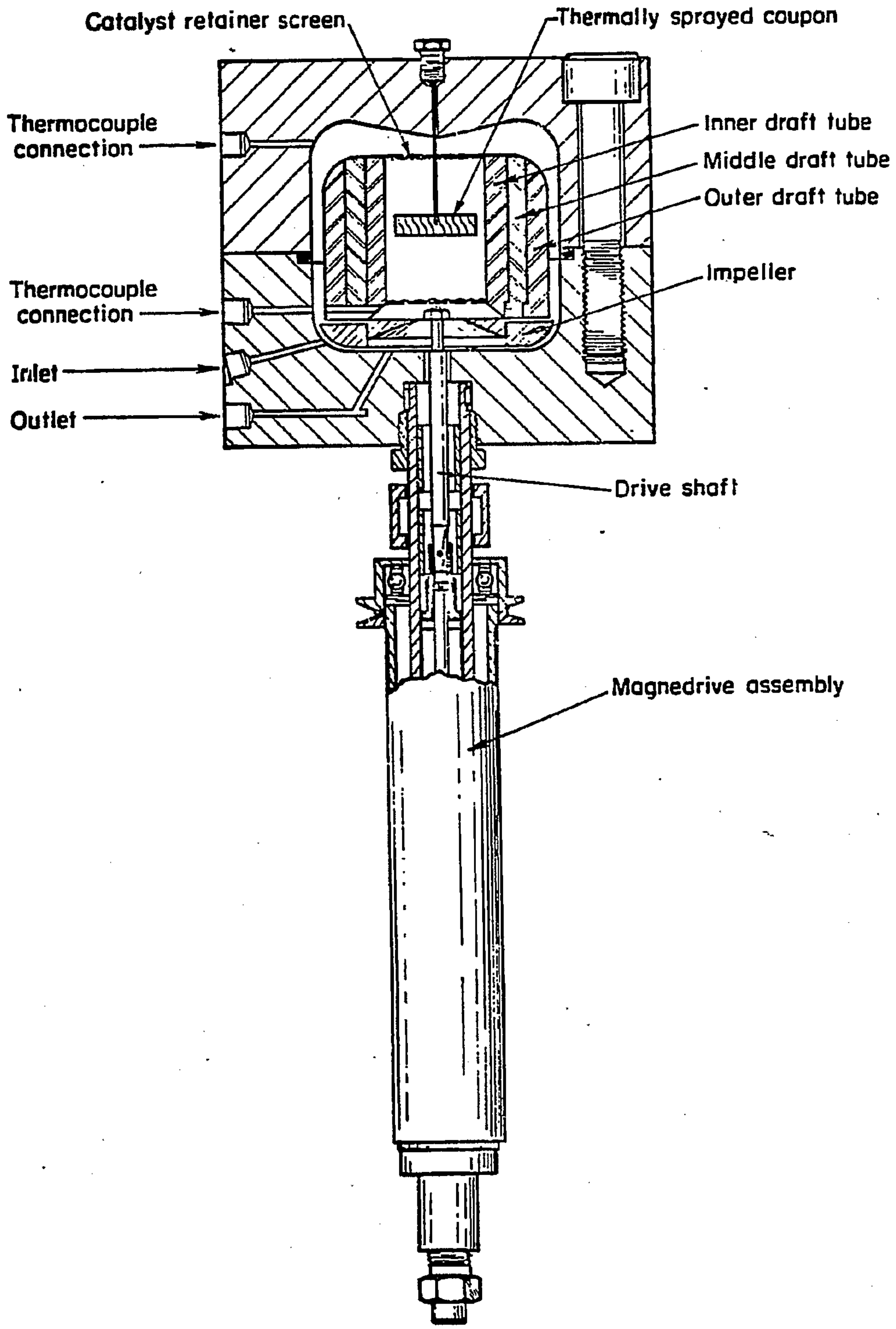

Figure 5. Berty reactor used for methanation kinetic studies

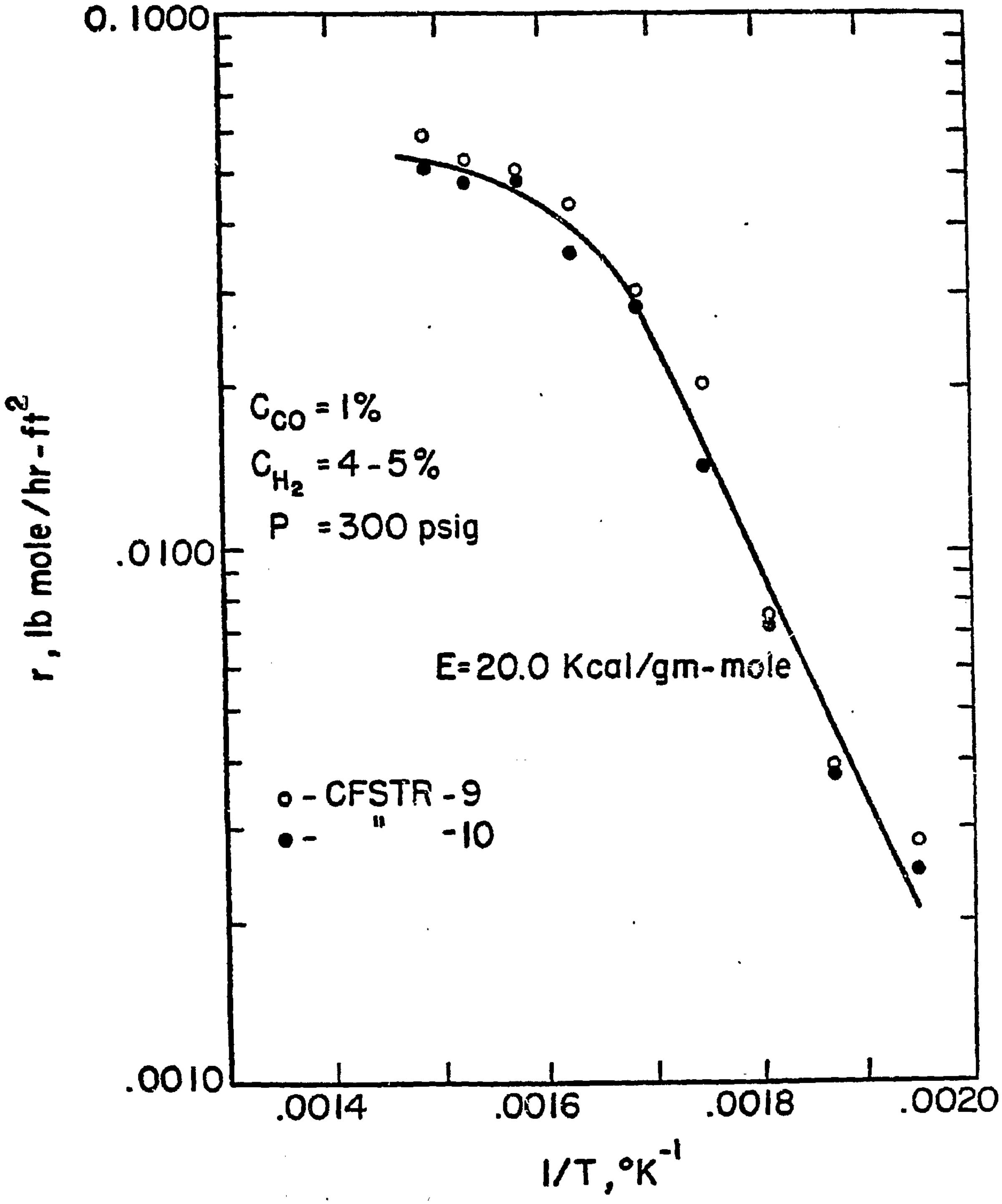

Figure 6. Arrhenius diagram for flame-sprayed Raney nickel

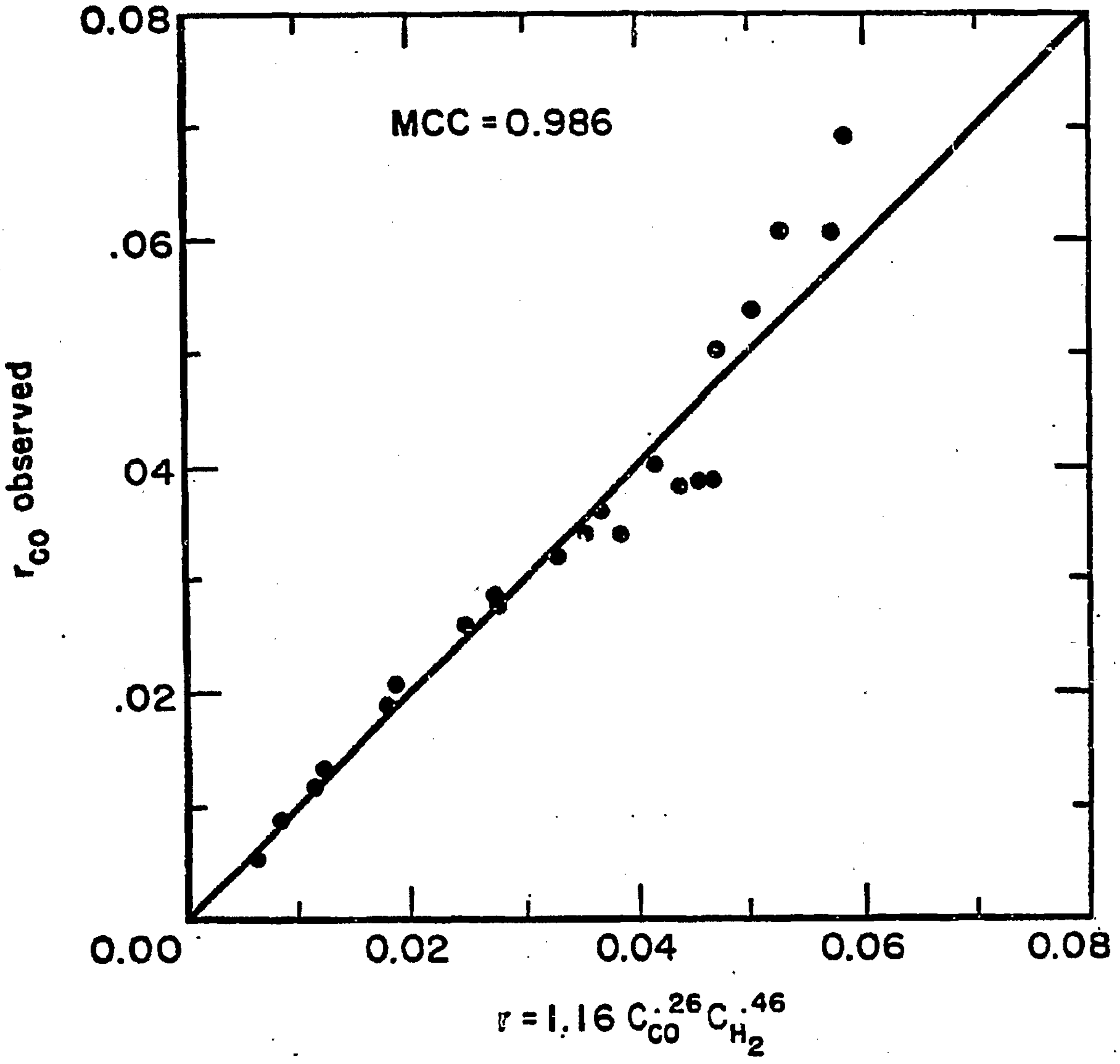

Figure 7. Parity plot illustrating the fit of experimental data to the kinetic regression equation.

3-14-78 L-15942

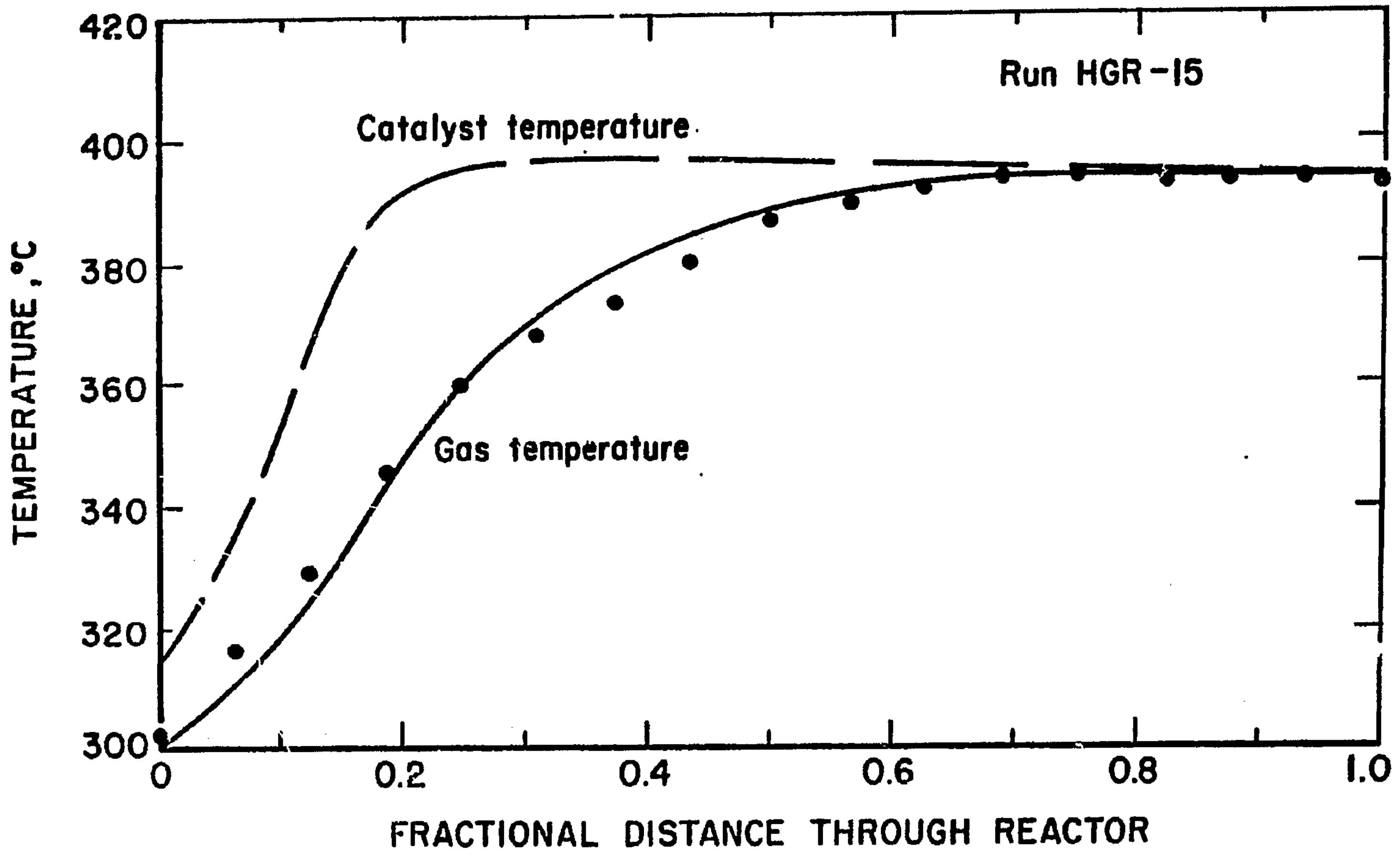

Figure 8. Temperature profiles for a Hot Gas Recycle Process Development Unit.

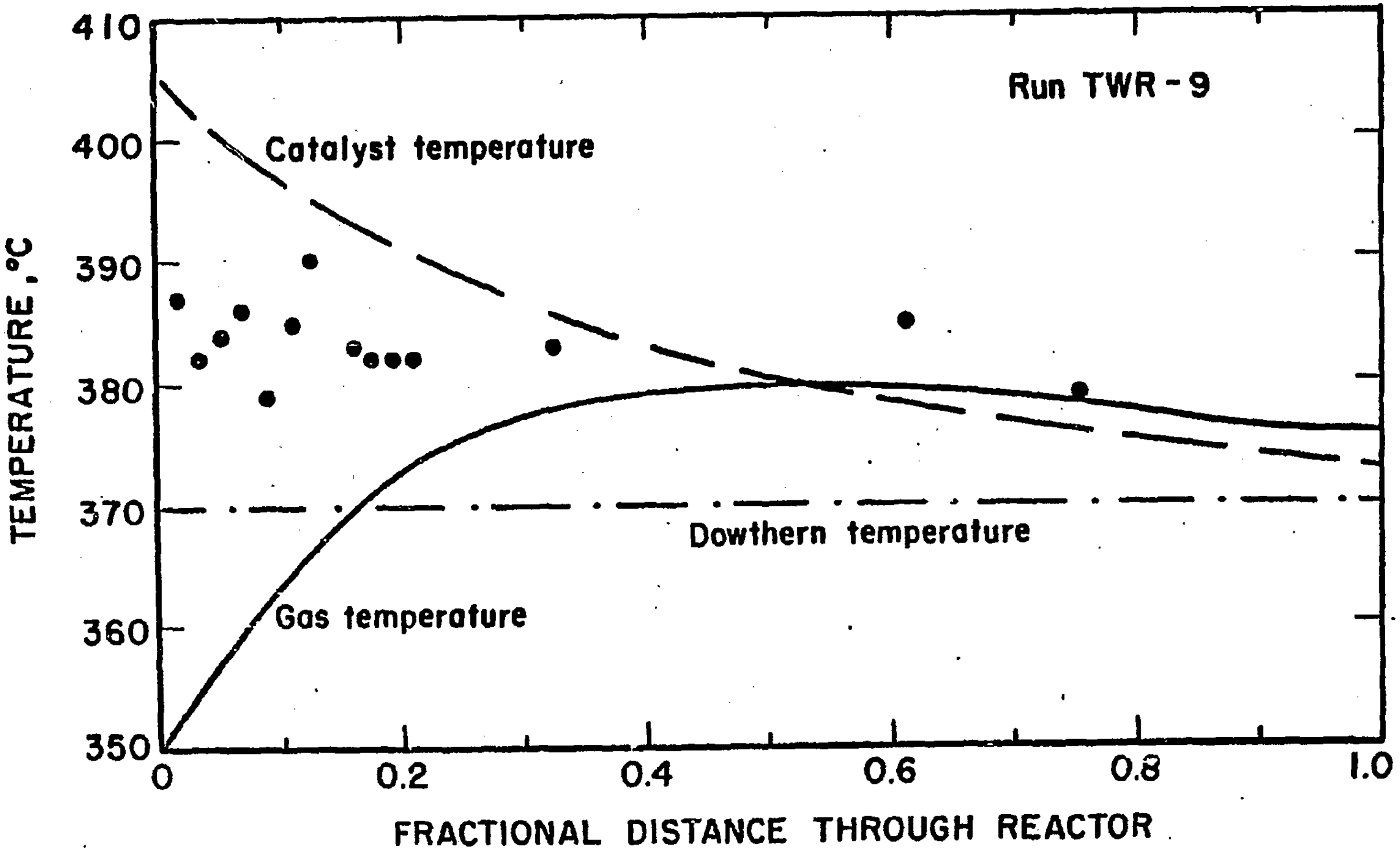

Figure 9. Temperature profiles for a Tube Wall Process Development Unit.

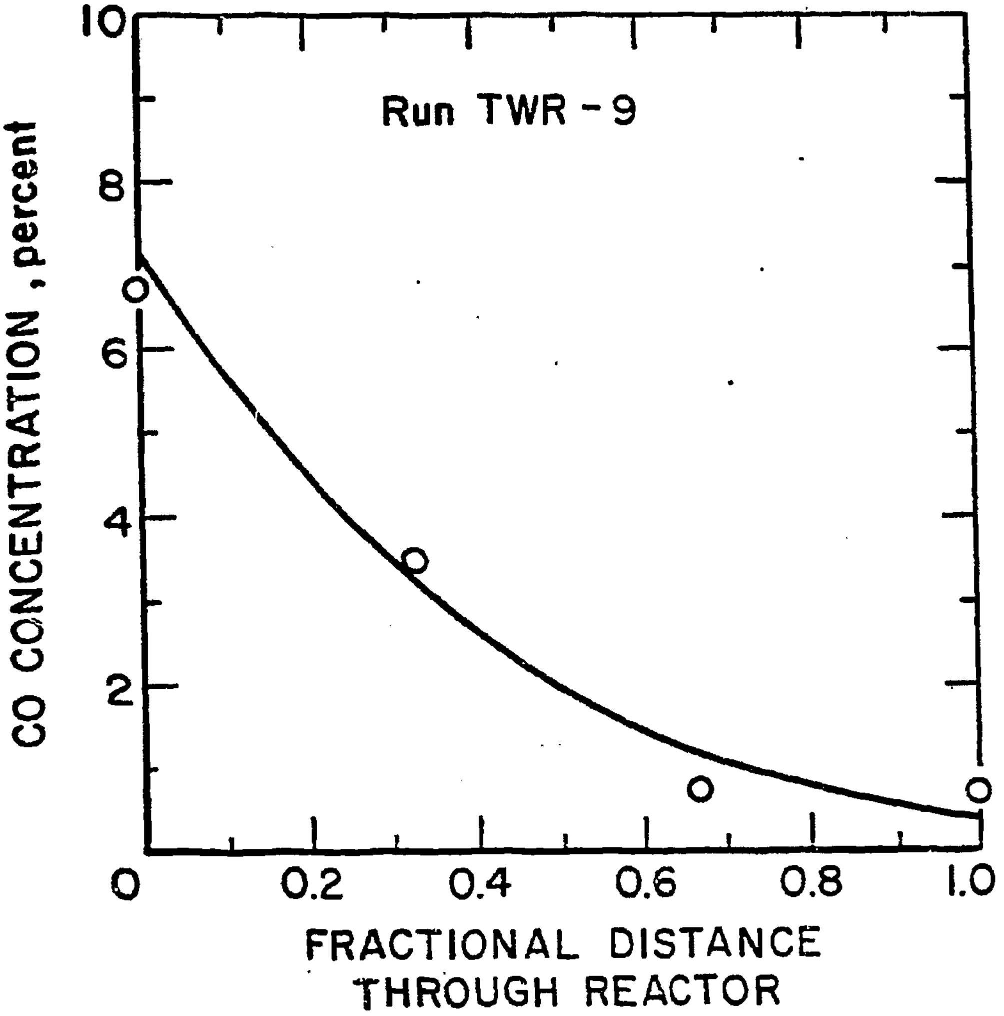

Figure 10. Concentration profile for a Tube Wall Process Development Unit.

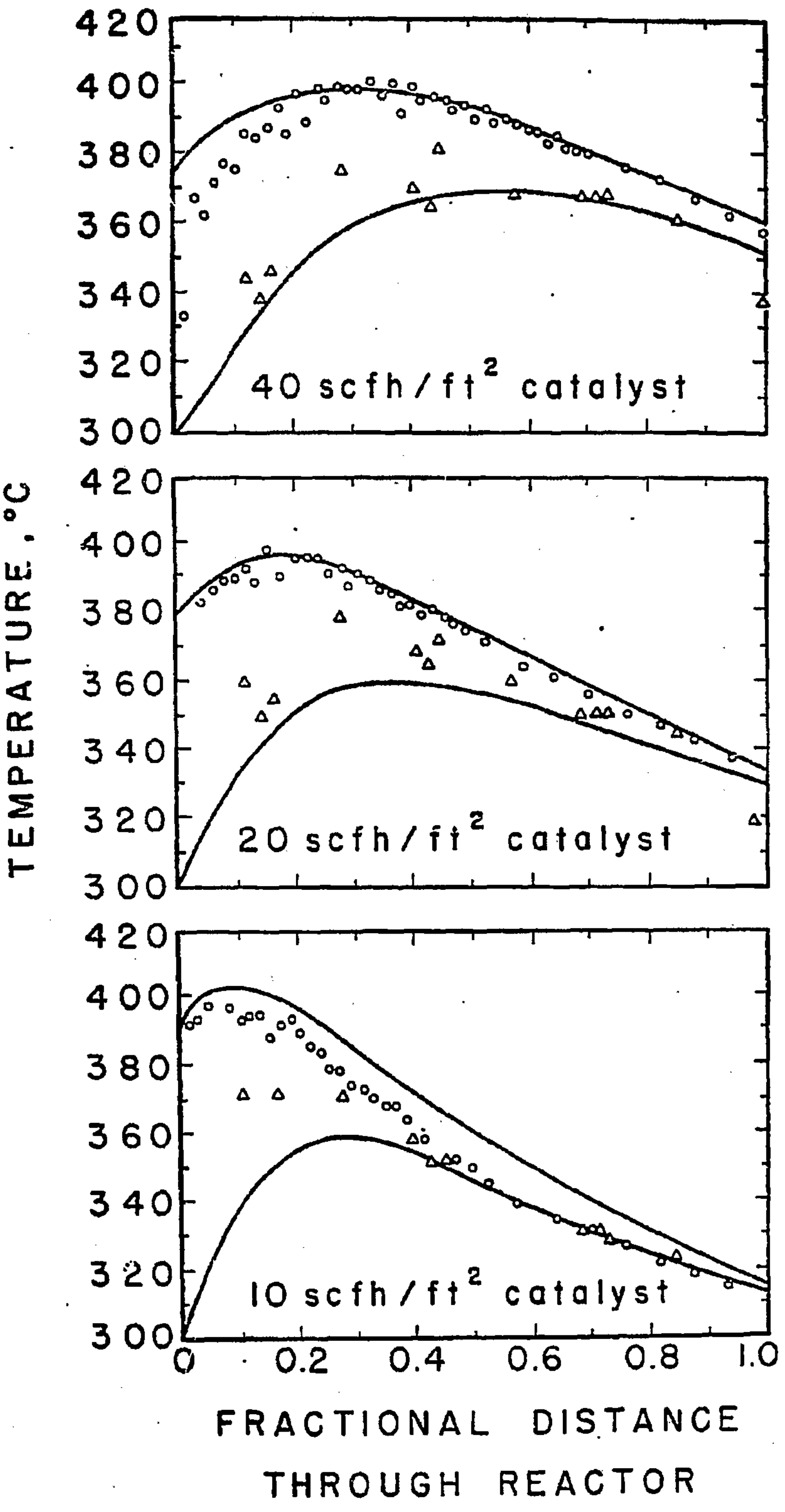

Figure 11. Temperature profiles for a Hybrid Process Development Unit for three different exposure velocities.

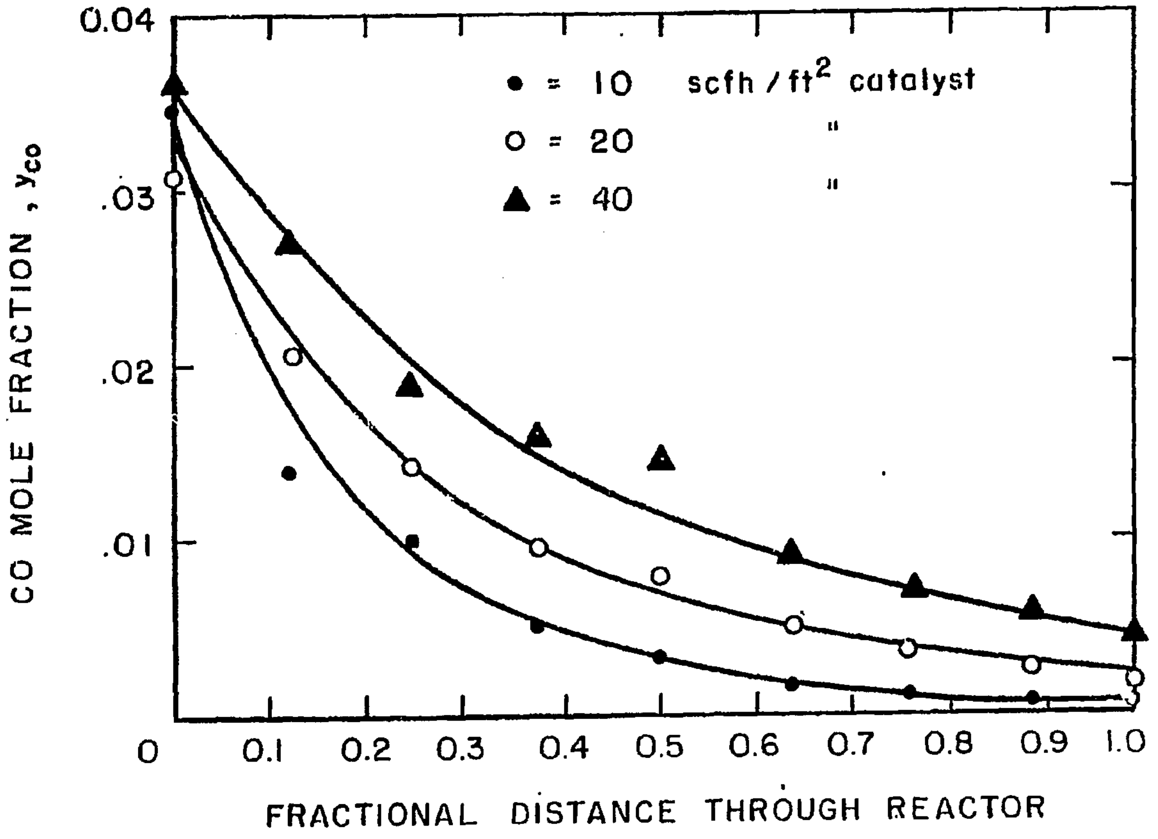

Figure 12. Concentration profiles for a Hybrid Process Development Unit for three different exposure velocities.

4-12-76 L-14779

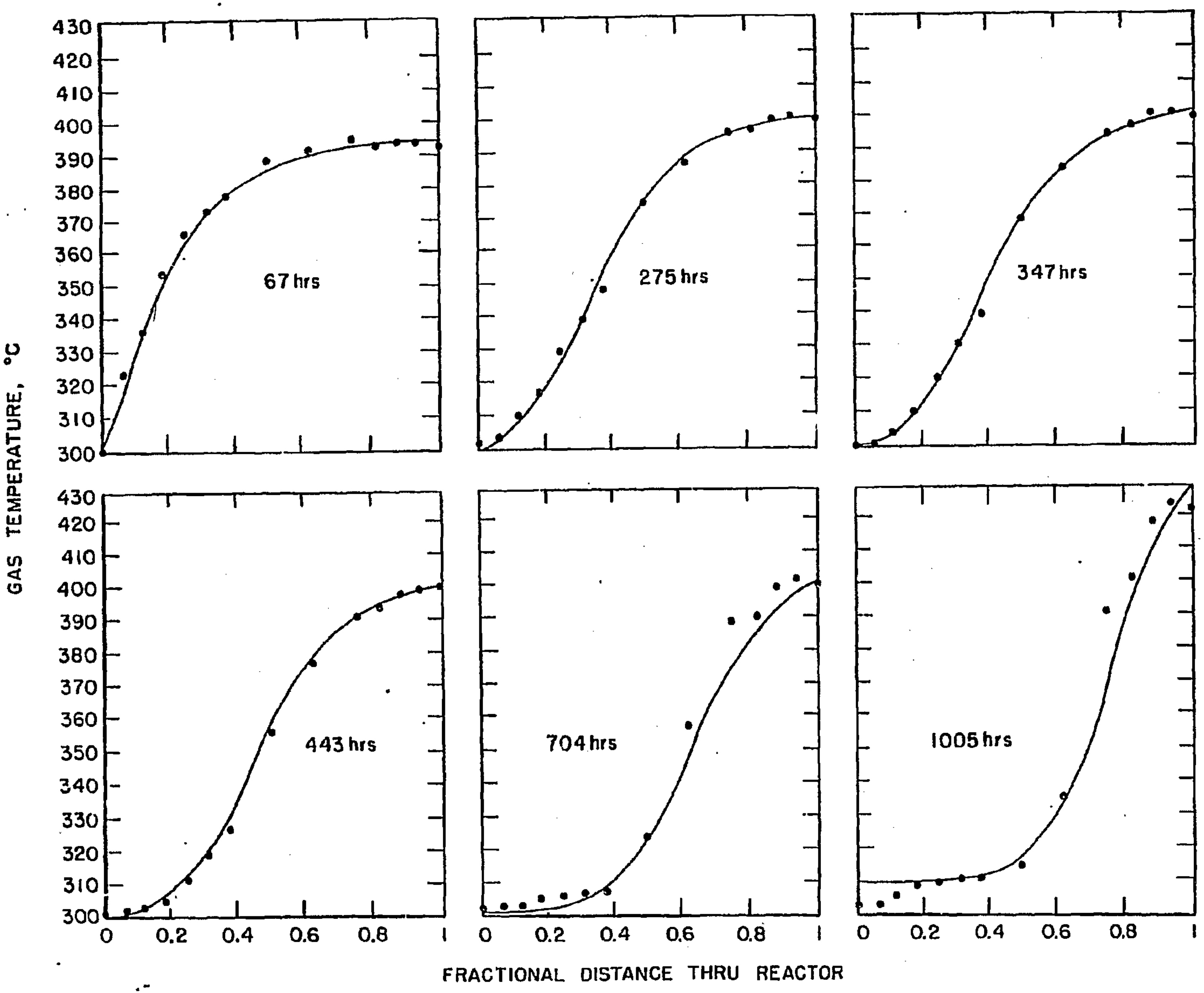

Figure 13. Gas temperature profiles of a Hot Gas Recycle Process Development Unit for different times on stream.

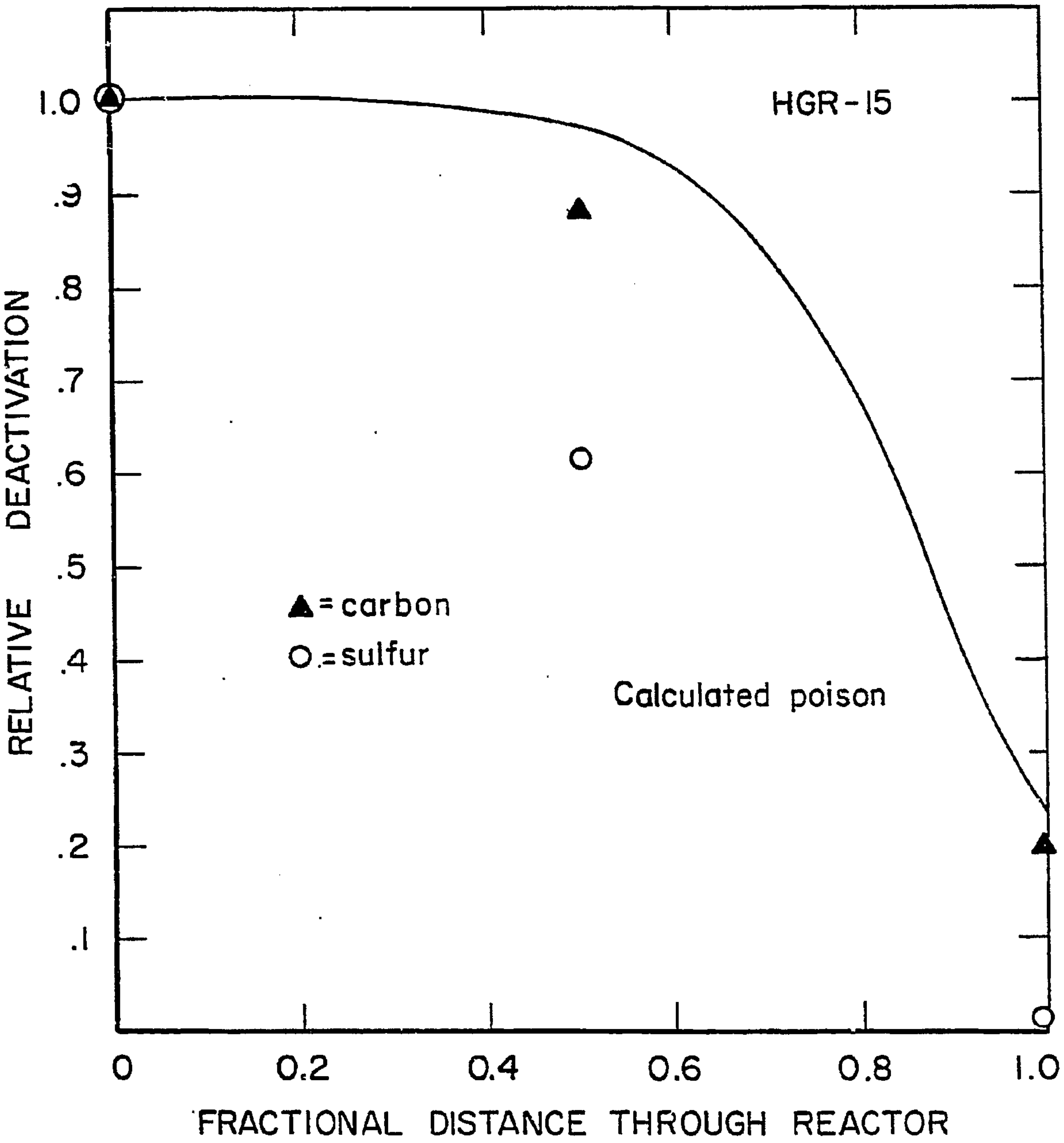

Figure 14. Poison profiles from Run HGR-15.